

CHAPTER 3

APPARATUS

Much of the apparatus used in the experiments described in this thesis was inherited from the previous PNC measurement. Intricate details of the apparatus will not be repeated where they have been presented in the literature or in previous theses, such as for the Pound-Drever-Hall locking scheme that stabilizes the dye laser to the power build-up cavity, or the details of the external cavity diode lasers used in the optical pumping and detection.

The entire apparatus fits onto a large optical table that is isolated from building vibrations by nitrogen-filled legs. A vacuum chamber, which is a large aluminum box measuring about $30 \times 56 \times 66$ cm is bolted to one end of the optical table. Figure 3.1 is a schematic of the apparatus showing the vacuum chamber on the right and the other assorted elements above and to the left. Cesium comes out of an oven in an atomic beam and enters the vacuum chamber. The atomic beam then enters the optical pumping region where the atoms are placed in a single hyperfine state by the hyperfine pumping laser. The atoms then enter the interaction region where there are mutually orthogonal electric, magnetic, and laser fields. The laser field is an intense standing wave with a wavelength of 540 nm. The standing wave is created in a Fabry-Perot etalon with a finesse of 10^5 . This etalon increases the power available to drive the $6S \rightarrow 7S$ transition in the cesium atoms and it is called the power build-up cavity (PBC). The 540 nm light is provided by a tunable dye laser that is locked to the PBC using the Pound-Drever-Hall method [32, 33]

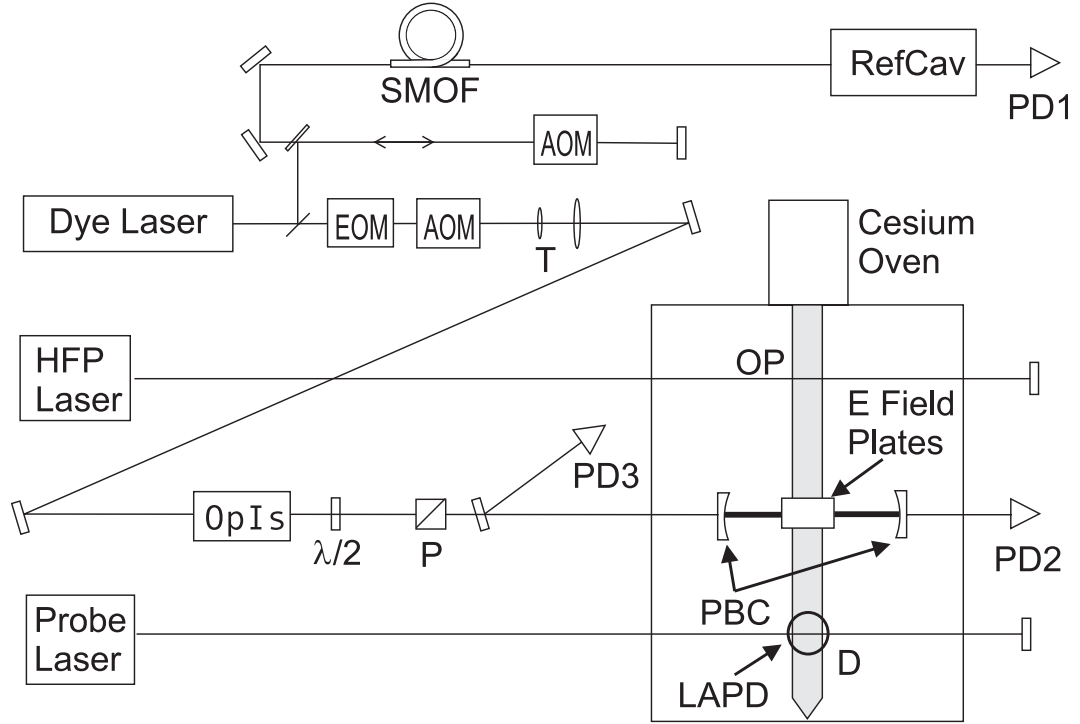


Figure 3.1: The apparatus used in the experiments described in this thesis. SMOF is a single-mode optical fiber, RefCav is the invar reference cavity, AOM is an acousto-optic modulator, EOM is an electro-optic modulator, T is a mode-matching telescope, HFP is the hyperfine-pumping diode laser, OP is the optical pumping region, OpIs is an optical isolator, $\lambda/2$ is a half-wave plate, P is a polarizer, PBC is the power build-up cavity, D is the detection region, and LAPD is a large area photodiode. PD1, PD2, PD3 are photodiodes.

and the PBC is then locked to a stable reference cavity. The atomic beam finally enters the detection region where atoms that repopulated the depleted hyperfine state after making the $6S \rightarrow 7S$ transition scatter photons from the probe laser. The scattered photons are collected on a large area photodiode, and the photocurrent is proportional to the number of atoms that made the $6S \rightarrow 7S$ transition. A schematic view of just the atomic beam path is shown in Fig. 3.2.

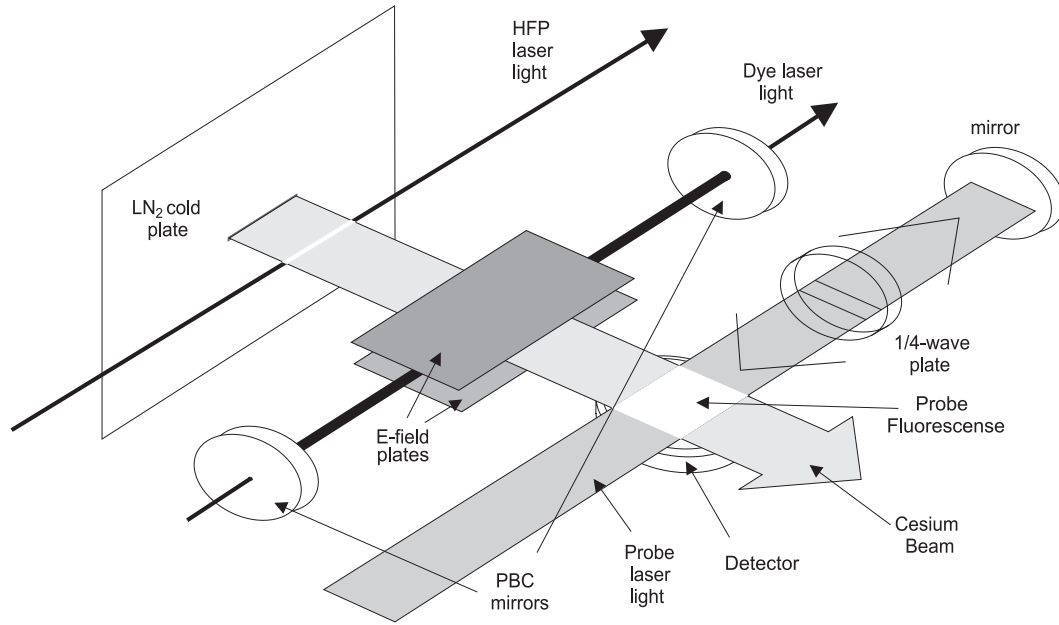


Figure 3.2: Detail of the atomic beam path showing its travel from the liquid nitrogen (LN_2) cooled plate, through the optical pumping region, through the interaction region, and into the detection region.

3.1 The Cesium Oven

The cesium oven used as the source of the atomic beam in these experiments was designed by Carl Wieman and built by Blaine Horner in the JILA instrument shop. It replaces the oven that had been used since the first PNC experiments with cesium were performed by Sarah Gilbert at the University of Michigan [20]. A diagram of the oven is shown in Fig. 3.3. The oven has two sections, the main section in the back of the oven where ampoules of cesium are placed and heated, and the nozzle in the front where the atoms receive their initial collimation.

To load the oven, its pieces are completely assembled except for the rear flange. Then, in a glove box back-filled with argon gas so that the cesium does not react with air, two 10 g cesium ampoules are broken and placed in a small glass “boat.” The boat is then placed in the main section of the oven and the rear flange is attached. The oven is then removed from the glove box and attached to the vacuum

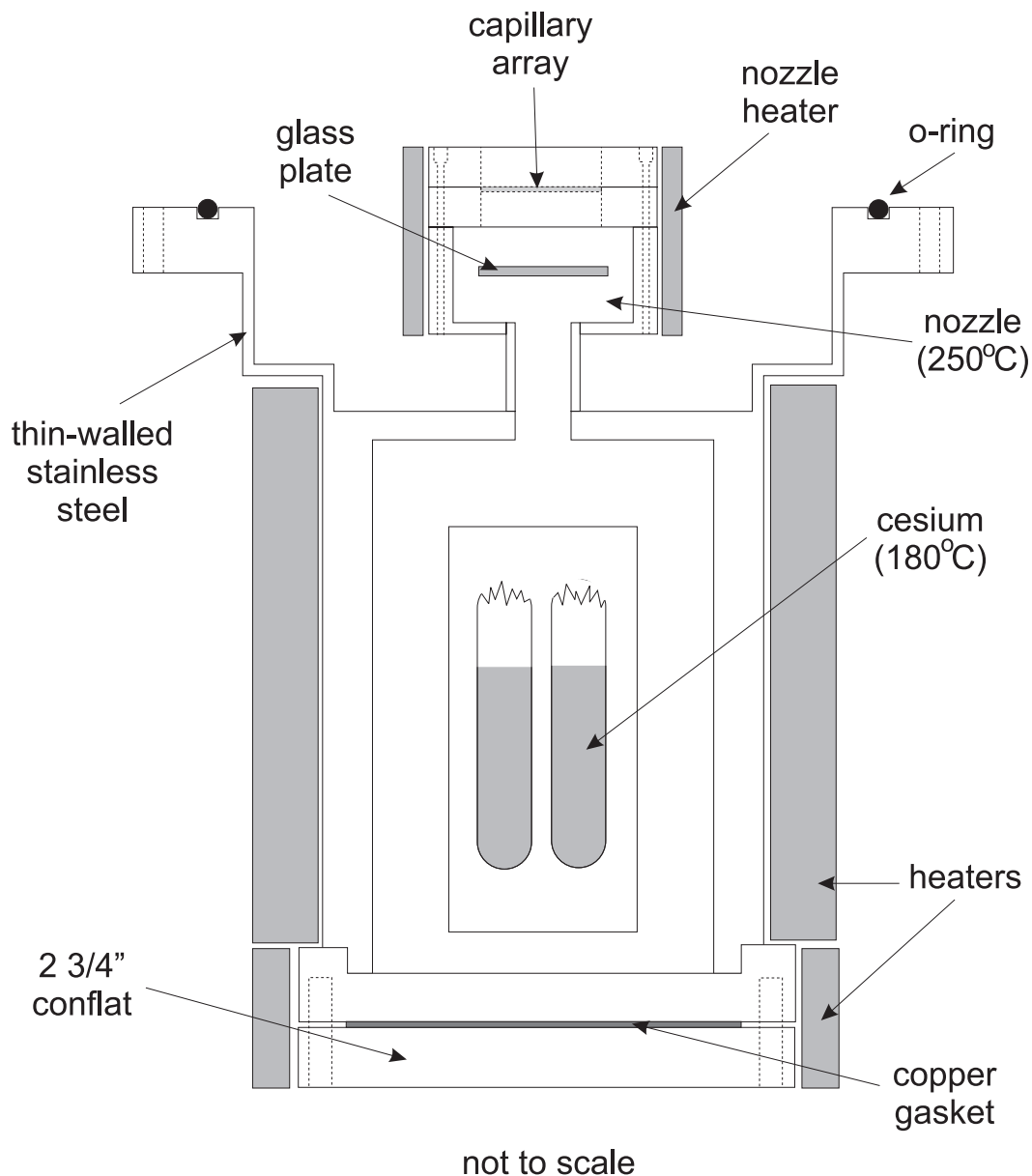


Figure 3.3: A schematic of the cesium oven. Shown are the back section where the cesium ampoules are loaded, the nozzle where the atoms rethermalized to $\sim 250^\circ\text{C}$, and the assorted heaters, capillary array, etc.

chamber. When the vacuum chamber has been evacuated, the oven gate [34] can be opened. The rear section of the oven is heated by two ceramic heaters fastened around the oven. The entire oven is then wrapped in insulation and temperature

stabilized at around 180°C.

The hot cesium atoms travel from the back of the oven through a small tube to the nozzle which is kept at 250°C to dissociate cesium dimers. A glass plate blocks the direct line-of-sight from the rear of the oven so that the atoms must rethermalize to the nozzle temperature. Once rethermalized, the atoms can leave the nozzle through a glass capillary array that is purchased from Galileo Electro-optics. The arrays are made from blocks of many glass tubes 10 μm in diameter, close packed, and sliced into 0.5 mm thick, 2.54 cm square wafers. Each wafer is then cut into 0.85×2.54 cm rectangles by dragging the corner of a razor blade across its surfaces until enough glass has been scraped away for the array to break cleanly along the scratch. The array covers an opening in the nozzle that is 0.8 cm high and 2.5 cm wide, which gives the initial definition to the atomic beam shape. After leaving the oven, the atomic beam passes through an aperture ~ 0.5 cm high \times 2.5 cm long in a large copper plate, which is cooled to liquid nitrogen (LN_2) temperature, and then the beam passes through a vertical vane collimator with vane separation of 1 mm. After the vane collimator the beam has a divergence of ~ 30 μrad .

It is important to note that capillary arrays are also sold as “microchannel plates”, which are made of leaded glass. These plates are often intentionally cut on a bias. That is, the slices are not cut normal to the long direction of the glass tubes. The arrays we received from our supplier varied in the angle at which they were cut from zero to five degrees, despite our specification of zero bias angle. To ensure a high flux in the atomic beam, we measured the bias angle of every array and rejected any arrays that had a bias angle of greater than 0.5°. We were able to use 65% of the arrays delivered to us.

3.2 Optical Pumping Region

Once collimated by the capillary array and the vane collimator, the atomic beam enters the optical pumping (OP) region, which is 10 cm from the oven. Here

the atoms interact with the hyperfine pumping laser (HFP), which is tuned to the $6S_{1/2}$ to $6P_{3/2}$ transition. We use the $F = 3$ to $F' = 4$ transition to deplete the $F = 3$ state when we want to drive transitions from the $6S_{1/2}$ $F = 4$ hyperfine state and we use the $F = 4$ to $F' = 3$ transition to deplete the $F = 4$ when we want to drive transitions from the $6S_{1/2}$ $F = 3$ hyperfine state. These transitions were chosen in previous experiments [22] to minimize the amount of light scattered down the beam that could “undo” the initial optical pumping and to minimize the number of atoms left in the depleted state. The requirements remain the same for the present experiments, so the hyperfine pumping scheme has not been changed.

The hyperfine pumping takes place in a 2.5 G magnetic field, and the polarization of the light is linear and perpendicular to the magnetic field. The light is therefore equal parts σ^+ and σ^- so that atoms should not be preferentially pumped to $m_F < 0$ or $m_F > 0$ states.

The HFP is an external cavity diode laser constructed using an SDL 5401-G1 semiconductor laser locked to a saturated absorption spectrometer as described in Ref. [35]. This laser provides approximately 20 mW/cm² of light, which is well above the 1.1 mW/cm² saturation intensity of cesium.

In previous experiments, the atomic beam was spin polarized as well as pumped into a single hyperfine state. That “Zeeman pumping”, which placed all the atoms into an extreme Zeeman sublevel, is not needed or used for the present experiments.

The result of this mechanical and optical manipulation is a well collimated beam of atoms predominantly (99.95%) in one hyperfine level of the ground state. The horizontal distribution of the atoms is fairly uniform with 64% of the atoms in the center 50% of the beam. The vertical distribution is roughly Gaussian with a height of ~ 0.8 cm. Typical fluxes were 10^{13} atoms/sec, estimated from the shot noise on the signal. (See Section 3.5.3 of Ref. [23] for a discussion of this estimation.)

3.3 Interaction Region

3.3.1 Electric and Magnetic Field Production

In the interaction region the atoms encounter a region of mutually orthogonal electric, magnetic, and laser fields. The electric field is produced by two plates, made either of molybdenum evaporated on glass or of solid molybdenum (depending on the experiment). The plates are centered on both the atomic beam and on the laser field. The magnetic field is produced mainly by a pair of Helmholtz coils, which is also centered on the atomic beam and the laser beam. The laser field is produced by a dye laser coupled into a high-finesse Fabry-Perot etalon as discussed below.

3.3.2 Dye Laser

The $6S \rightarrow 7S$ transition is excited by a 540 nm laser field. For the previous PNC experiment and for the present experiments, the frequency of the laser driving the $6S \rightarrow 7S$ transition must be extremely stable. To achieve the necessary stability, we use the locking scheme shown in Fig. 3.4. The dye laser is a heavily modified Spectra-Physics 380 pumped by a Coherent Innova-90 argon ion laser. Typical ion laser powers range from 3 to 5 W, depending on the age of the dye, and give 200-500 mW of tunable, single-frequency 540 nm light. We use a dye solution made of 1 g/ ℓ of Pyromethene 556 dye dissolved in ethylene glycol.

Coarse tuning of the laser is accomplished using an intracavity birefringent tuner, while thick and thin etalons select the longitudinal lasing mode. A Faraday rotator prevents bidirectional lasing. Fine tuning of the laser frequency is performed using three additional intracavity elements. Two galvanometer-mounted glass plates with a range of about 20 GHz control the frequency on a slow time scale ($f < 2$ Hz). A piezoelectric transducer behind one of the cavity mirrors has a range of approximately 300 MHz and controls the frequency at an intermediate time scale ($2 \text{ Hz} < f < 2 \text{ kHz}$). Finally, an electro-optic modulator controls the frequency at

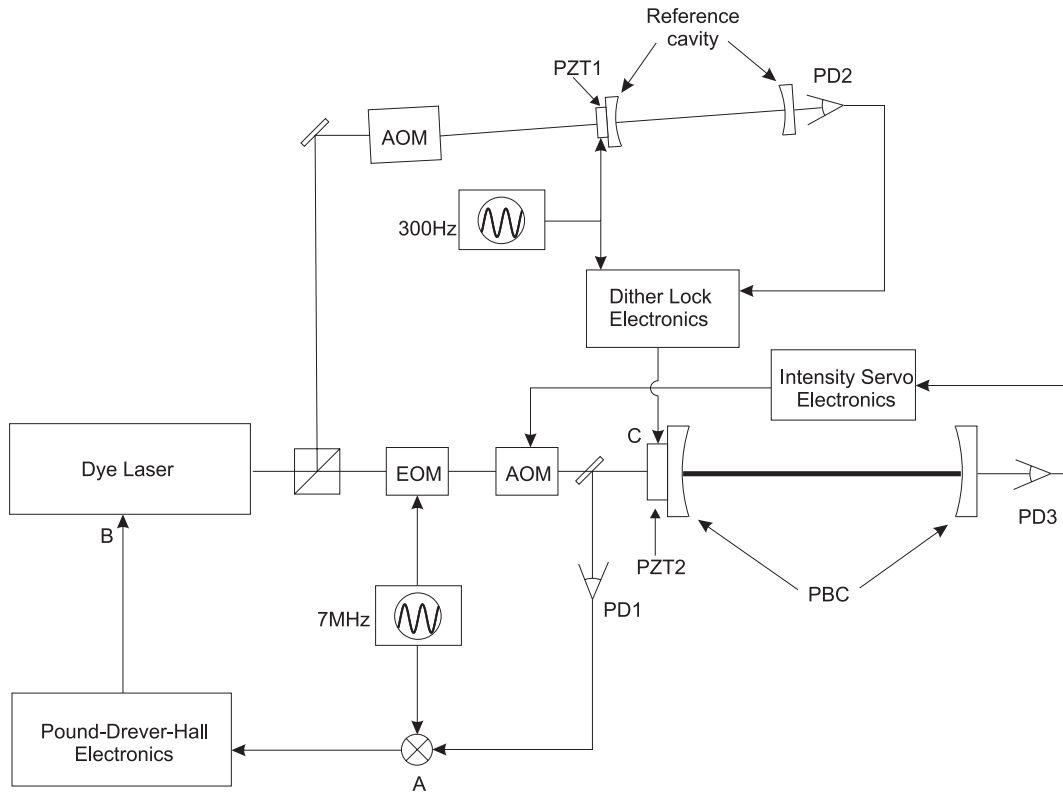


Figure 3.4: A schematic of the dye laser frequency stabilization scheme. The dye laser passes through the EOM where it is phase modulated at 7 MHz and through an AOM before entering the PBC. The light reflected off the PBC is directed to a photodiode (PD1). The signal from PD1 is mixed with the 7 MHz driving signal at A to generate an error signal. The error signal is sent to the Pound-Drever-Hall electronics and then to the dye laser transducers at B. The dye laser is also sent through a second AOM to the reference cavity. The input piezo-electric transducer (PZT) is dithered at 300 Hz. The modulated transmission of the reference cavity is collected on PD2 and sent to the dither lock electronics where an error signal is generated and sent to the PBC PZT at C. The transmission of the PBC collected on PD3 is used to stabilize the intensity of the dye laser.

fast time scales ($\sim 1.3 \text{ MHz} > f > 2 \text{ kHz}$).

The gross location of the dye laser frequency is referenced to a group of molecular iodine lines. The proper mode of the laser can be found by scanning the frequency of the laser and observing the fluorescence in an iodine cell. If the laser is far away from the correct frequency it is sometimes necessary to use a portable

scanning double monochromator to set the frequency of the laser near 540 nm.

3.3.3 Fast Frequency Stabilization

The light from the dye laser passes through an electro-optic modulator that puts 7 MHz sidebands on the light. The light then passes through an acousto-optic modulator used to stabilize the laser intensity. The light passes through a telescope for proper mode matching into the etalon. An optical isolator protects the laser from optical feed back, and a half-wave plate and a polarizer are used to control the polarization. The laser light is then incident on the Fabry-Perot etalon.

The frequency of the dye laser is locked to the etalon using the Pound-Drever-Hall method [32]. This method works by looking at the 7 MHz sidebands reflected off the input mirror of the etalon after they are demodulated on a photodiode. When the laser frequency is directly on the resonance of the etalon, the sidebands are phase shifted by equal and opposite amounts. The two sidebands sum together and the demodulated signal size is zero. When the dye laser frequency is slightly detuned from resonance, the sidebands are not phase shifted equally and the demodulated signal is nonzero. Thus, an error signal can be derived from the demodulated sum of the sidebands and used to feed back to the galvos, the piezo and the EOM in the dye laser to keep the frequency of the dye laser on the etalon resonance. When locked to the etalon the dye laser has a line width much less than the 5 kHz resonance width of the etalon.

3.3.4 Power Build-up Cavity

The Fabry-Perot etalon is constructed of two high reflectivity multilayer dielectric mirrors 2.5 cm in diameter. The input mirror has a radius of curvature of 10 m and the output mirror has a radius of curvature of 6 m. The two mirrors are separated by 27 cm, which gives the etalon a free spectral range of $\simeq 550$ MHz and a relatively large beam radius of $\omega_0 = 0.41$ mm. Since the etalon geometry is almost

“flat-flat” there is minimal focusing of the beam. In fact, the beam waist only varies by 1% over the length of the etalon.

The two mirrors are of very high quality with the transmittance of each expressed in parts per million rather (ppm) than per cent. The input mirror has $T = 40$ ppm and the output mirror has $T = 13$ ppm. The geometry and the reflectivity combine to give the etalon a finesse of 10^5 , and the power inside the etalon is approximately 30,000 times the incident power. For this reason, the etalon is referred to as the power build-up cavity (PBC), and it is one of the main reasons the experiments described in this thesis and the PNC experiment are possible at all. The power density inside the cavity is typically 800 kW/cm^2 , which makes observation of the very weak $6S \rightarrow 7S$ transitions easy.

The mechanical design of the PBC is shown in Fig. 3.5. The two mirrors are mounted on aluminum brackets using silicone rubber to minimize stress-induced birefringence. The brackets are then mounted in optical mounts. The input mirror is also mounted to a tube piezo-electric transducer (piezo) to allow for tuning of the

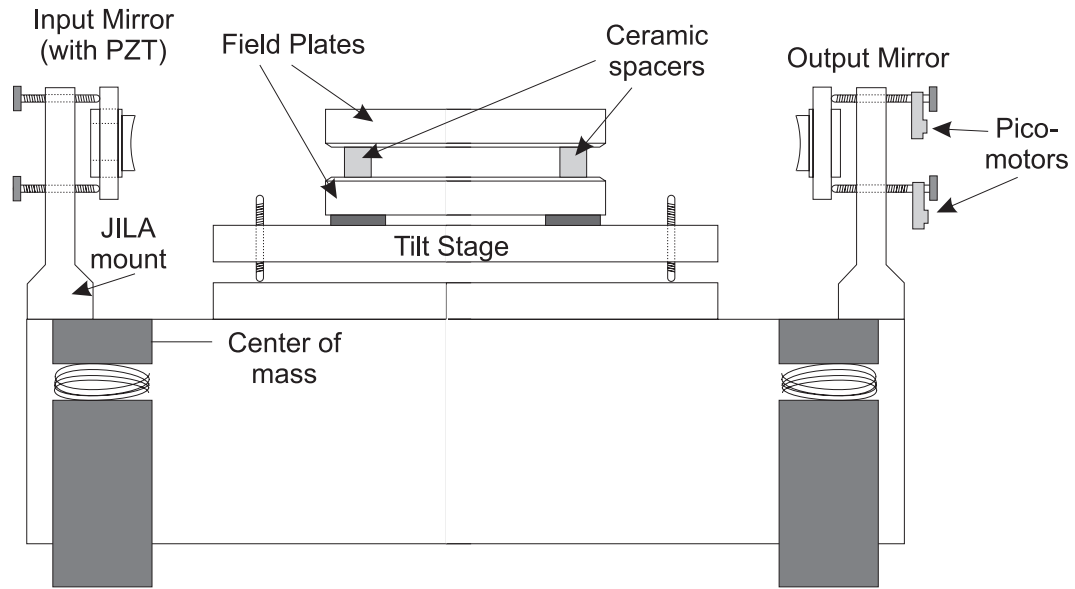


Figure 3.5: Detailed mechanical design of the PBC.

resonant frequency of the PBC. The two mounts are then bolted to a large granite block, which is very rigid and provides a large inertial mass. The granite block is suspended in the plane of its center of mass by four beryllium-copper springs, which are damped by a small amount of sorbothane rubber. This arrangement is to minimize tilts between the cavity and the optical table and to retain a gentle suspension to isolate the cavity from vibration and shock. Since temperature variations will cause frequency shifts, both mirror mounts are temperature stabilized.

3.3.5 Slow Frequency Stabilization

While the line width of the dye laser is less than 5 kHz on a short time scale when locked to just the PBC, the PBC does bounce slightly, and the piezo on the input mirror can creep. Therefore the longer term stability can be unacceptably poor. In order to stabilize the frequency of the dye laser on long time scales, the PBC is locked to a stable reference cavity. This reference cavity was locked to the peak of the $6S \rightarrow 7S$ transition for the PNC experiment, and was only used to stabilize the PBC on a long time scale. However, for the experiments described in this thesis the cavity must serve as a frequency reference by itself.

To improve the stability of the reference cavity, which is already constructed of Invar, the nearly confocal cavity was hermetically sealed, and a second stage of temperature stabilization was added. In addition, light is coupled into a single mode optical fiber before going into the reference cavity because motion of the beam incident upon the reference cavity can cause a change in the point at which the PBC locks to the reference cavity. (See Chapter 4.)

One of the mirrors of the reference cavity is mounted on a piezo. The voltage on this piezo is dithered at 300 Hz, and the transmission through the cavity is monitored on a lock-in amplifier. The signal from the lock-in amplifier provides an error signal that is fed back to the PBC piezo, and thus the PBC is kept locked to the reference cavity.

3.4 Detection Region

After the atoms interact with the frequency-stabilized dye laser light and are excited to the $7S$ state they relax back to the $6S$ state via transitions to the $6P_{1/2}$ and $6P_{3/2}$ states and then to the ground state. The atoms decay to both hyperfine states of the ground state with 75% of the atoms decaying to the state with the same quantum number F to which they were excited. That is, of the $7S_{1/2}$ $F' = 4$ atoms, 75% decay to the $6S_{1/2}$ $F = 4$ and 25% decay to the $6S_{1/2}$ $F = 3$. We then detect the number of atoms that made the $6S \rightarrow 7S$ transition by “counting” the number of atoms that are in the initially depleted hyperfine state.

To detect atoms that relax to the $F = 4$ hyperfine state we lock another external cavity diode laser—the probe laser [23, 35]—to the $6S_{1/2}$ $F = 4$ to $6P_{3/2}$ $F' = 5$ transition. Since the dipole selection rule requires $\Delta F = 0, \pm 1$, atoms driven to the $6P_{3/2}$ $F' = 5$ state can only relax back to the $6S_{1/2}$ $F = 4$ (since there are no $F = 5$ or 6 states in the ground state) where they are available to be excited again. We collect roughly 200 scattered photons per atom on this “cycling” transition on a large area photodiode located directly beneath the region where the atomic beam and probe beam intersect. We place a gold mirror above the atomic beam to reflect photons emitted upward back into the photodiode. In order to maximize the number of photons an individual atom can scatter we use two cylindrical telescopes to widen the probe laser beam to about 2.5 cm in width and 1 cm in height.

The situation is a little different for atoms that are excited out of the $F = 4$ hyperfine state. The appropriate cycling transition here is the $6S_{1/2}$ $F = 3$ to $6P_{3/2}$ $F' = 2$. This transition suffers from the problem that it is similar to a “lambda” transition where there are fewer excited state levels than there are ground state levels. Atoms that are excited can eventually evolve into a superposition of ground states are no longer resonant with the excitation recitation; they “go dark” [36, 37, 38].

In order to prevent the atoms from “going dark”, the probe beam is linearly

polarized and reflected back upon itself, passing twice through a quarter wave plate. The result is that the polarization of the reflected light is rotated by 90° forming a configuration known as “lin-perp-lin” [39], which has a spatial variation of the polarization. At one point in space the light is linearly polarized, then $\lambda/8$ away the light is σ^+ polarized, then another $\lambda/8$ away the light is linearly polarized, then σ^- , and so on. In addition, a magnetic field gradient is applied in the detection region so that as an atom moves down the atomic beam it is in a different magnetic field each time it is excited to the $6P_{3/2}$ state. In this way the atoms never encounter the right conditions to “go dark.” The scheme is not perfect, however, and the number of photons scattered on the $F = 3$ to $F' = 2$ transition is only 45% of the number scattered on the $F = 4$ to $F' = 5$ transition

3.5 Data Acquisition

All of the work presented in this thesis is basic spectroscopy. That is, the frequency of the dye laser is scanned across the $6S \rightarrow 7S$ transition, and the transition rate as a function of laser frequency is recorded. A computer controls the data acquisition in the following manner, schematically illustrated in Fig. 3.6.

The computer sends a signal to a digital-to-analog converter that provides a control voltage to change the frequency of the dye laser. For low-precision measurements of the line shape (Section 7.1) the computer changes the voltage on the reference cavity piezo, thus changing the reference frequency. For the dc Stark shift measurement (Chapter 4) and for the tensor transition polarizability measurement (Chapter 5) the computer controls the frequency of an AOM that shifts the frequency of the light coupled into the reference cavity. The frequency of the dye laser must change to account for the shift.

After a fixed amount of time after the dye laser control voltage changes (to let transients settle, etc.), the computer triggers two gated integrators. These integrators integrate the signal from the probe photodiode and the voltage controlling

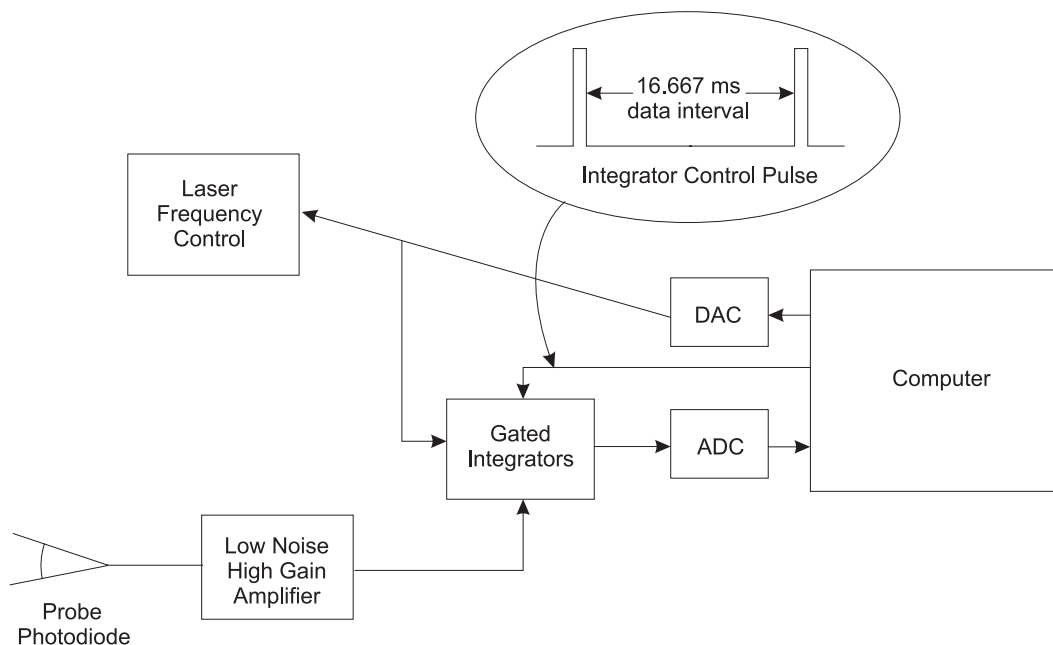


Figure 3.6: A schematic of the data acquisition system. The computer controls the laser frequency through a digital-to-analog converter (DAC). As the laser scans over the transition, the scattered light is collected on the probe photodiode (PPD) and amplified. The voltage to the frequency control and the signal from the PPD are integrated in 16.667 ms intervals, converted on the analog-to-digital converter (ADC) and stored on disk.

the laser frequency. The length of the integration interval, which is also controlled by the computer, is 16.667 ms. This particular interval is chosen to average away any 60 Hz noise. The two voltages are then converted to a digital signal by an analog-to-digital converter and are stored on disk. As the control voltage is scanned, we generate a transition rate versus voltage plot that, with suitable calibration, may be converted to a transition rate versus frequency plot similar to that shown in Fig. 3.7. Plots like this make up the data for all of the experiments described in this thesis.

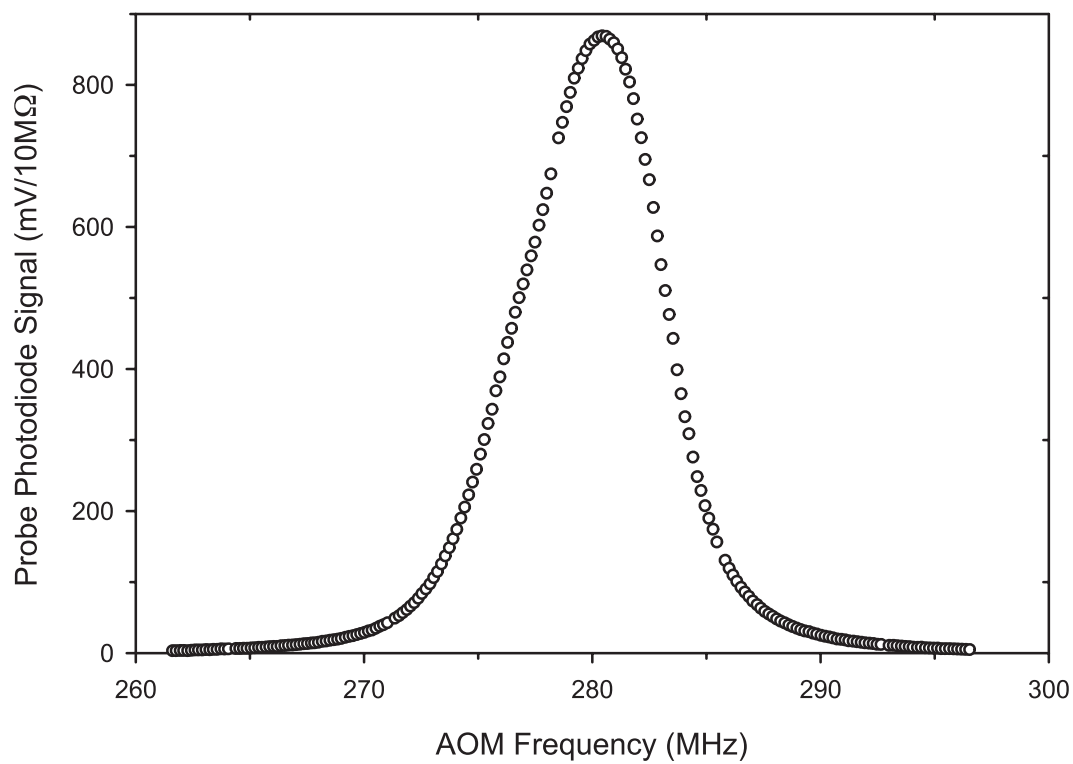


Figure 3.7: A sample of the data taken for the measurements in this thesis. The x-axis is the frequency of the AOM that shifts the frequency of the dye laser before it is incident on the reference cavity, and the y-axis is the signal from the probe photodiode.